Materials Chemistry and Physics 117 (2009) 74–79

Contents lists available at ScienceDirect

Materials Chemistry and Physics

journal homepage: www.elsevier.com/locate/matchemphys

Enhanced photocatalysis, colloidal stability and cytotoxicity of synchrotron X-ray synthesized Au/TiO_2 nanoparticles

Chi-Jen Liu[a], Tsung-Yeh Yang[a], Chang-Hai Wang[a], Chia-Chi Chien[a,b], Shin-Tai Chen[a], Cheng-Liang Wang[a], Wei-Hua Leng[a], Y. Hwu[a,b,c,d,*], Hong-Ming Lin[e], Yao-Chang Lee[d], Chia-Liang Cheng[f], J.H. Je[g], G. Margaritondo[h]

[a] *Institute of Physics, Academia Sinica, Nankang, Taipei 115, Taiwan*
[b] *Department of Engineering Science and System, National Tsing Hua University, Hsinchu 300, Taiwan*
[c] *Institute of Optoelectronic Sciences, National Taiwan Ocean University, Keelung 202, Taiwan*
[d] *National Synchrotron Radiation Research Center, Hsinchu 300, Taiwan*
[e] *Department of Materials Engineering, Tatung University, Taipei 10461, Taiwan*
[f] *Department of Physics, National Dong Hwa University, Hualien 97401, Taiwan*
[g] *X-ray Imaging Center, Pohang University of Science and Technology, Pohang, South Korea*
[h] *Ecole Polytechnique Fédérale de Lausanne (EPFL), CH-1015 Lausanne, Switzerland*

ARTICLE INFO

Article history:
Received 14 November 2008
Received in revised form 10 March 2009
Accepted 2 May 2009

Keywords:
Nanostructure
Biomaterials
Electron microscopy
Visible and ultraviolet spectrometers

ABSTRACT

Au/TiO_2 nanocomposite particles were synthesized by a method based on intense X-ray irradiation without adding any reducing agent or stabilizer. The nanocomposite exhibits promising photocatalytic and biological properties at physiologically relevant concentration ([Au] = 0.028 mM, [TiO_2] = 0.5 mM). The structure and photocatalysis were examined by X-ray diffraction, electron microscopy and ultraviolet–visible spectroscopy demonstrating that gold nanoparticles of 2–5 nm size were successfully deposited on TiO_2 nanoparticle surfaces. The nanocomposite exhibited good colloidal stability within a typical cellular environment and was nontoxic to cancer cell according to evaluations under controlled conditions. The Au/TiO_2 nanoparticles were also found to enhance the photocatalytic efficiency of UV radiation and even more that of X-ray radiation. In vitro studies indicated that the cell-killing effect under X-ray irradiation is more pronounced with the addition of Au/TiO_2 nanoparticles than of bare TiO_2 nanoparticles.

1. Introduction

The photocatalytic efficiency of TiO_2 nanoparticles is an important performance factor for their practical applications in areas such as solar cells [1], sanitation [2] and cancer therapy [3]. This efficiency can be improved by adding Au [3–5], Ag [6,7] or Pt [7,8] to their surface. To guarantee the effectiveness of this approach, the metal coating cannot completely cover the substrate photocatalytic surface and should be in the form of small nanoparticles. The surfaces of both TiO_2 and of the metal nanoparticles must be optimized to achieve maximum efficiency. This is not trivial with solution chemistry [9,10] and gas phase condensation methods [11].

We present here the successful synthesis of such nanocomposites by a non-conventional X-ray irradiation method and the characterization of the results in view of possible phototherapeutical applications. The first demonstration was for Au nanoparticles on TiO_2 nanoparticles. Au is indeed particularly interesting because of its biocompatibility and of its enhancements of the radiation response [12,13].

Most formation processes for the Au-TiO_2 nanocomposite are based on reducing precursor gold ions on the pre-formed TiO_2 nanoparticles. By adapting a recently developed one-step X-ray irradiation synthesis method of Au nanoparticles [14–17], the Au-TiO_2 nanocomposite synthesis could be achieved with no additional reducing agent, organic solvent or stabilizer. The nanocomposite so produced exhibits good colloidal stability and size uniformity that enabled us to prepare high concentration solutions with high biocompatibility and excellent colloidal dispersion.

The high intensity of synchrotron X-rays produced a synthesis yield order of magnitude larger than other photosynthesis methods. A detailed characterization of the nanocomposites revealed other positive features such as the uniformity of the nanoparticle size and of the distribution in the nanocomposite, as well as the possibility of precise fabrication control.

In view of possible applications to radiation cancer treatment, we analyzed the colloidal stability within the cellular environments

* Corresponding author. Tel.: +886 2 2789 6721.
E-mail address: phhwu@sinica.edu.tw (Y. Hwu).

0254-0584/$ – see front matter © 2009 Elsevier B.V. All rights reserved.
doi:10.1016/j.matchemphys.2009.05.030

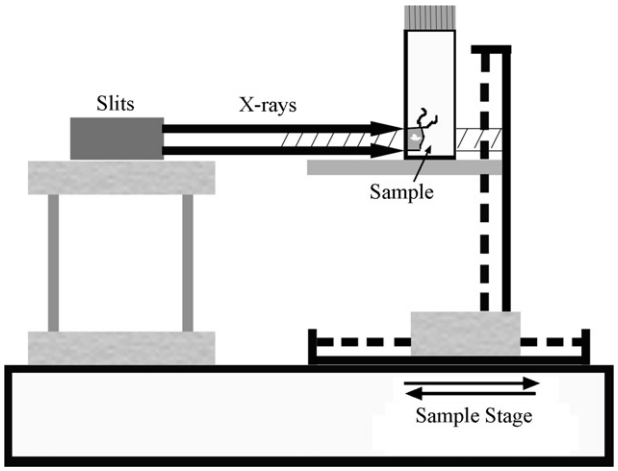

Fig. 1. Scheme of our experimental setup.

and the cytotoxicity of our Au/TiO_2 nanoparticles. We found higher colloidal stability and enhanced cell-killing effect with X-ray irradiation than that of unmodified TiO_2 nanoparticles and nontoxicity up to 0.5 mM as far as the EMT-6 cell line is concerned.

Cancer treatments based on photocatalytic process were already realized. In vivo animal studies confirmed remarkable effectiveness [18,19]. In previous studies of photodynamic therapy (PDT), most authors used metal oxide semiconductor materials with ultraviolet (UV) irradiation. However, UV light is affected by serious problems: its penetration is low and it is difficult to focus. Highly penetrating X-ray radiation is promising for the treatment of cancers in deep organs without optics fibers or surgery. Notwithstanding the potentially negative effects of a large dose, X-rays are already widely used in standard therapeutical procedures. Furthermore, we already proved that X-ray irradiation is very effective in activating TiO_2 nanoparticles in solution (data not shown).

We explored the impact of the addition of Au nanoparticles to the TiO_2 surface on the photocatalytic effectiveness of both UV radiation and X-rays. We found that in both cases the effectiveness is enhanced, as demonstrated by measurement of the decomposition of methylene blue (MB) [20].

The possibility of therapeutic applications is enhanced by the high biocompatibility of the Au/TiO_2 nanoparticles and by other factors. Note in particular the use of an aqueous solvent instead of the organic solvents (e.g. acetonitrile or toluene) for chemical reduction methods and the absence of reductants and stabilizers, resulting in better compatibility for biological applications. In addition, the exposure time to obtain fully reduced Au nanoparticles is much shorter than with conventional chemical [10] and photochemical [7] approaches or even γ-ray radiation-induced synthesis [21].

2. Experimental

2.1. Nanoparticle preparation

Au/TiO_2 nanoparticles were synthesized by an X-ray irradiation method similar to our previous works [16,17], with some modifications. Typically, 0.01 g of commercial P25 TiO_2 (anatase phase, specific surface area $50 \pm 15\ m^2\ g^{-1}$, average primary particle size 21 ± 3 nm, purity > 99.5%) were added to 10 ml of de-ionized water to prepare a well-mixed TiO_2 nanosol. A well-mixed aqueous solution containing 0.02 M of gold precursor (hydrogen tetrachloroaurate trihydrate, $HAuCl_4 \cdot 3H_2O$, Aldrich) with an appropriate amount of NaOH (0.1 M) was subsequently added while stirring. The resulting solution was then exposed to a high flux of X-ray photons at the BL01A beamline of the Taiwan National Synchrotron Radiation Research Center (NSRRC)—where an unmonochromatized beam is emitted by a 4.5 T wavelength shifter with a broad photon energy distribution from 8 to 15 keV, centered at ~12 keV [22]. The schematic experimental setup is shown in Fig. 1. The synthesis time was used to control the size of the Au nanoparticles and typically ranged from few seconds to few minutes.

To evaluate the photocatalytic properties of Au/TiO_2 nanoparticles, analytical grade MB was used as a model dye. 0.4 ml TiO_2 or Au/TiO_2 nanosol were added to 10 ml of de-ionized water (18.2 MΩ cm, Millipore, Milli-Q, MA, USA) or RPMI medium with 10% serum mixed with MB, producing the desired concentration of the TiO_2 or Au/TiO_2 nanosol (0.5 mM). Before irradiation, each nanosol was magnetically stirred in the dark for 15 min to reach the adsorption/desorption equilibrium. The photocatalytic studies were performed using X-rays from the same NSRRC beamline, with different exposure times (5, 10, 15, 20 s).

2.2. Characterization

2.2.1. Synchrotron powder X-ray diffraction (SP-XRD)

XRD measurements were implemented on the BL17A wiggler beamline of NSRRC at the X-ray wavelength of 0.1333 nm. The diffraction signal was accumulated for 15 min and recorded by an imaging plate 0.12 m from the sample. The spectrum was converted to the equivalent Cu Kα (1.5418 Å) radiation spectrum for JCPDS indexing. The Au/TiO_2 samples for diffraction were prepared by drying concentrated colloidal solution drops overnight in a pumped dessicator. The nanocrystalline size was estimated by the broadening of the diffraction peaks using Scherrer's formula with a *K*-value of 0.9.

2.2.2. Transmission Electron Microscopy (TEM)

The structure, morphology and size of nanoparticles were examined by a field emission electron microscope (FE-TEM, JEOL, JEM-2100F) operating at 200 KV with a LaB6 filament and with Energy Dispersive X-ray Spectroscopy (EDXS) module including an ultra-thin window X-ray detector and an Oxford Instruments Plc. computer system. The samples for TEM analysis were prepared by putting droplets of nanoparticles containing solution on carbon-coated Cu grids and allowing them to dry at ambient atmosphere. The size of immobilized Au nanoparticles was derived by analyzing more than 30 particles.

2.2.3. UV–vis absorption spectra

The photocatalytic effects of TiO_2 and Au/TiO_2 nanoparticles activated by synchrotron X-ray irradiation were evaluated by a UV–vis spectrometer (GBC UV-160). The absorbance of the remaining MB in the mixture was measured at the wavelength of 664 nm in the UV spectrum after each irradiation. The concentration of MB was quantitatively evaluated using a calibration graph constructed using reference solutions at different concentrations.

2.2.4. Dynamic light scattering (DLS)

The variations of the hydrodynamic size of colloidal TiO_2 and Au/TiO_2 nanosols in DI water or in an RPMI (Royal Park Memorial Institute culture medium, Gibco) medium containing 10% fetal bovine serum (FBS) were monitored during up to 4 h by a DLS size analyzer (Horiba L-500, Horiba Inc., Japan). 0.4 ml of TiO_2 or Au/TiO_2 nanosol were added to 10 ml of water or medium producing the 0.5 mM TiO_2 or Au/TiO_2 nanosol.

2.3. Cell culture and MTT assay

EMT-6 cells were cultured in RPMI (GIBCO) medium containing 10% FBS, 1% antibiotics (penicillin at $100\ U\ ml^{-1}$ and streptomycin at $100\ \mu g\ ml^{-1}$) and L-glutamine at 37 °C in a humidified 5% CO_2 incubator. For MTT assay, MTT

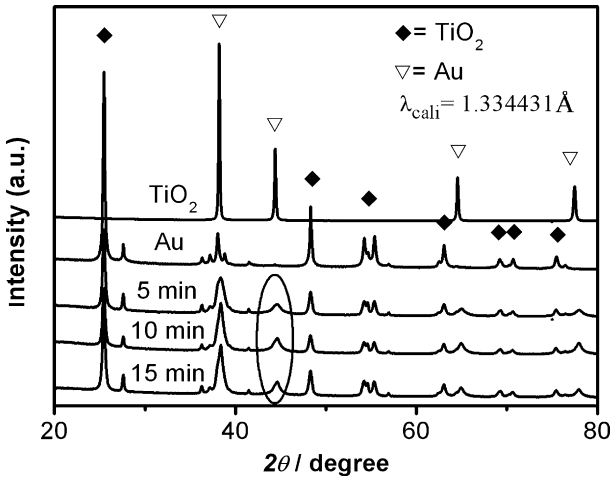

Fig. 2. SP-XRD diffraction patterns of anatase TiO_2 nanoparticles and pure Au nanoparticles, as well as synthesized Au/TiO_2 nanoparticles particles for X-ray exposure times of 5, 10 and 15 min.

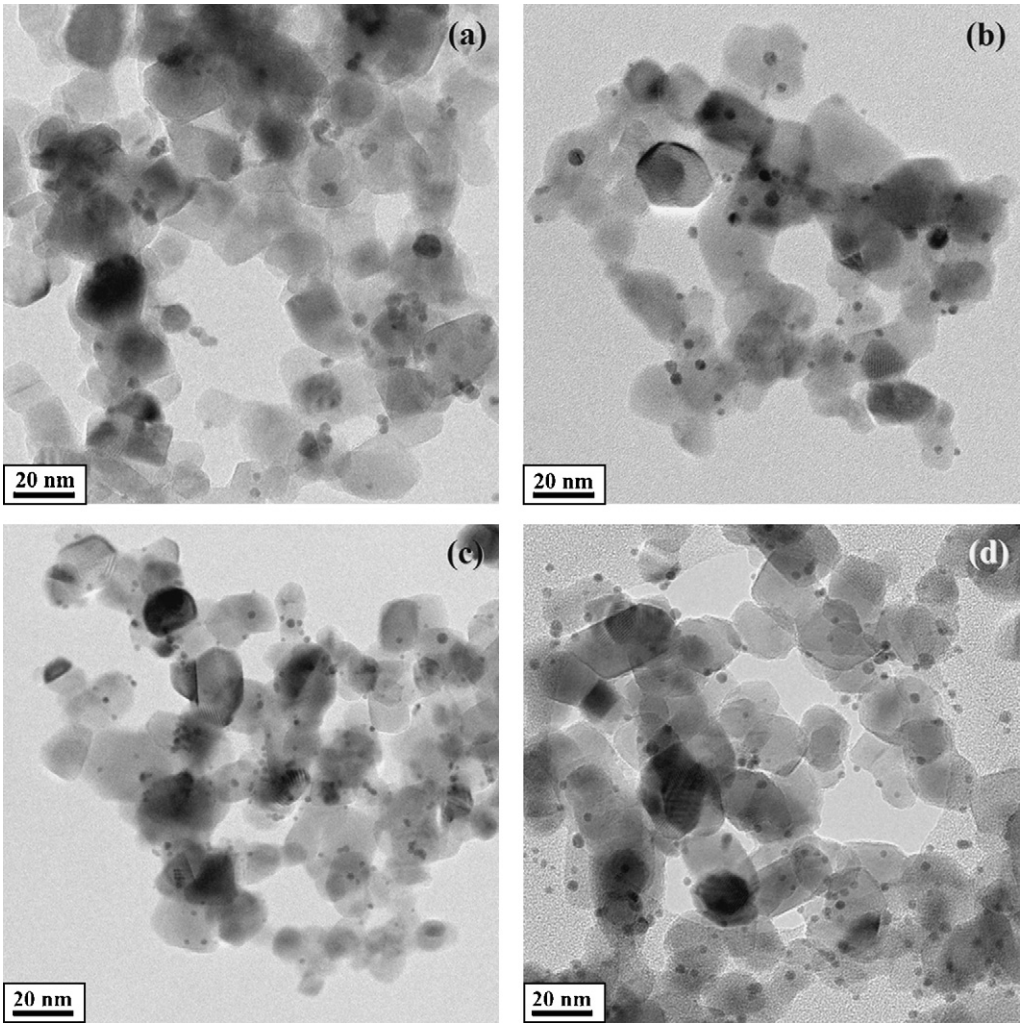

Fig. 3. TEM images of synthesized Au/TiO_2 nanoparticles for different X-ray exposure times. Labels: (a) 1 min, (b) 5 min, (c) 10 min, and (d) 15 min.

(3-[4,5-dimethylthiazol-2-yl]-2,5-diphenyltetrazolium bromide; Thiazolyl blue, Sigma–Aldrich, USA) reagent was dissolved in phosphate buffered saline (PBS, pH 7.4) and filtered through a 0.22 μm filter. EMTs were seeded within 24-well culture dishes before nanoparticle treatment. After seeding the cells for 24 h, the desired concentrations of TiO_2 or Au/TiO_2 nanosol were obtained and retained for 1 h, then washed with fresh medium, further incubated for 24 h, and subsequently used for the MTT assay. MTT solution was added to each well and incubated for 3–4 h.

Cellular reduction of MTT produces an insoluble, purple formazan. At the end of the incubation period the formazan crystals were dissolved in dimethyl sulfoxide (DMSO) and the absorbance at 570 nm was measured with a standard micro plate reader (Sunrise, Tecan, Switzerland). The quantity of formazan crystals as measured by the absorbance at 570 nm is directly proportional to the number of living cells in the culture. The relative cell viability (%) was calculated as $[A]_{test}/[A]_{control} \times 100$, where $[A]_{test}$ is the absorbance of the sample with gold nanoparticles and $[A]_{control}$ is that of the control sample without nanoparticles. Each experiment was performed three times. The cells thus prepared were irradiated by the monochromatized X-ray beam (6.5 keV in photon energy) obtained by appropriately tilting a single crystalline silicon wafer (1 0 0) with respect to the incident white X-rays at the BL01A beamline of NSRRC. The total dosage was measured [20], but we cannot exclude effects from a relatively small fraction of X-rays that are of higher energy and due to higher harmonics emission.

3. Results and discussion

3.1. Characterization of Au/TiO_2 nanoparticles

Detection of low intensity of diffraction signals from nanoparticles is challenging with a conventional powder X-ray diffractometer, but easier with the high flux and high brightness of a synchrotron X-ray source. Fig. 2 shows X-ray diffraction patterns of Au, TiO_2 and Au/TiO_2 nanoparticles for different exposure times (15, 10, and 5 min). The results demonstrate the desired structure and phase purity of the Au, TiO_2, and Au/TiO_2 nanoparticles.

The average Au particle size was derived from the broadening of the Au (1 1 1) reflection peak, obtaining 1.11, 0.98 and 0.83 nm for different Au/TiO_2 samples after X-ray exposure during 5, 10 and 15 min; the results suggest a decreasing trend. The average particle size of TiO_2 derived from the (1 0 1) TiO_2 reflection peak was the same (24–26 nm) for all the samples.

Note that whereas the accuracy of the XRD derivation of nanoparticle sizes is questionable, the statistical value for the overall nanocomposites is good. TEM was also used to confirm the size distribution and morphology of the Au nanoparticles. Fig. 3 shows a typical set of TEM images of Au/TiO_2 samples after drying in solution. These images confirm that the Au nanoparticles are uniformly formed on the TiO_2 surface. A short X-ray exposure time (1 and 3 min for Fig. 3(a) and (b)) leads to larger gold nanoparticles than a long one (10 and 15 min for Fig. 3(c) and (d)), consistent with the XRD results. The size of the Au nanoparticles was estimated to be 2–5 nm depending on the X-ray exposure time. For example, according to the TEM image processing analysis the size of the Au nanoparticles for 1 min X-ray exposure was 4.58 ± 1.06 nm, while for 15 min X-ray exposure it was 2.59 ± 0.88 nm. Au nanoparticles in this range exhibit high catalytic activity [23].

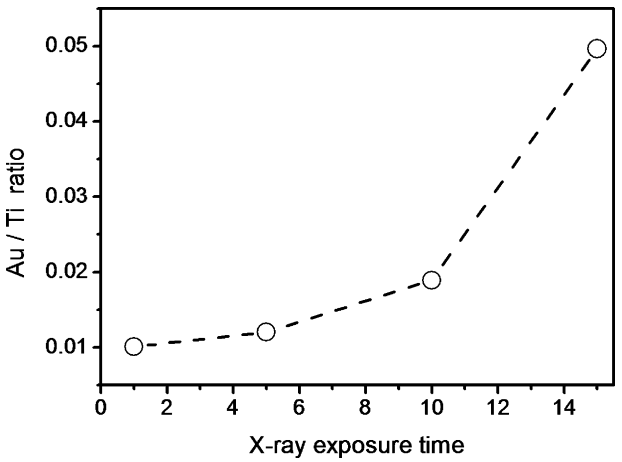

Fig. 4. Atomic ratio of Au/Ti for Au/TiO_2 nanoparticles as a function of the X-ray exposure time derived from TEM-EDXS analysis.

We also found that an increase in the irradiation time leads to a larger amount of Au nanoparticles on the TiO_2 surface. Semi-quantitative measurements were performed with EDXS and shown in Fig. 4. The average compositions were determined with three independent measurements. The atomic ratio of Au/Ti in synthesized Au/TiO_2 nanoparticles after X-ray exposure for 1, 5, 10 and 15 min were 0.010, 0.012, 0.019, and 0.050. Thus, the amount of Au nanoparticles on the TiO_2 was found to increase with the exposure time. In the following discussions, unless otherwise noted, "Au/TiO_2" refers to the particles formed with the optimum X-ray irradiation time of 15 min.

3.2. Comparison of the photocatalytic activity of TiO_2 and Au/TiO_2 nanosols

In view of the possible use for cancer treatment, the photocatalysis effectiveness of Au/TiO_2 nanoparticles with physiologically relevant concentration was investigated. The X-ray and UV photocatalytic enhancement induced by the Au nanoparticles was examined by UV–vis spectrometer. Fig. 5 shows the visible light MB spectral changes in the de-ionized water in the presence of TiO_2 nanosol or X-ray synthesized Au/TiO_2 nanosol (the initial concentration was TiO_2 = 0.5 mM; Au/TiO_2 = 0.028 mM/0.5 mM) after UV irradiation with a wavelength of 254 nm for 30 and 60 min. The

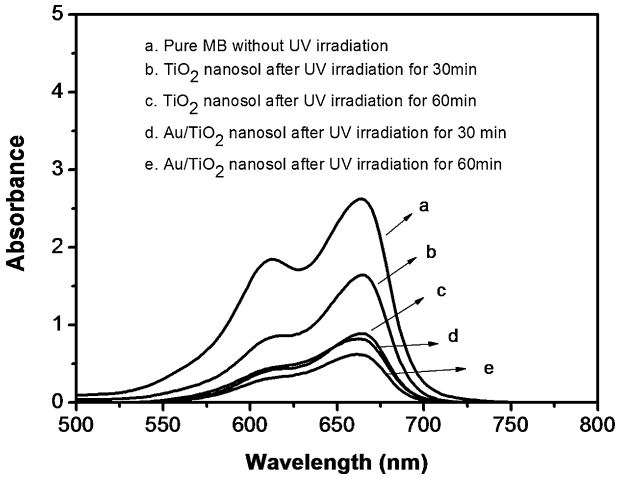

Fig. 5. Absorption spectral MB changes in the presence of TiO_2 or Au/TiO_2 (Au/Ti = 0.050) nanoparticles in de-ionized water. The initial concentrations were: MB = 0.25 mM; TiO_2 = 0.5 mM; Au/TiO_2 = 0.028 mM/0.5 mM.

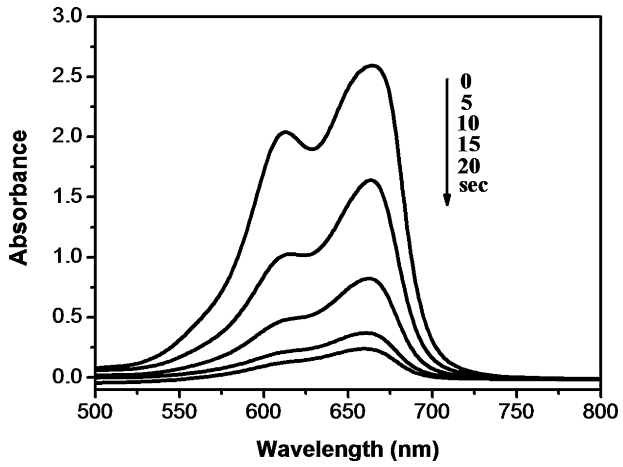

Fig. 6. Absorption spectral MB changes in the presence of TiO_2 nanoparticles in de-ionized water as a function of the X-ray irradiation time. The initial concentrations were: MB = 0.25 mM; TiO_2 = 0.5 mM.

decrease in the absorbance at 664 nm reflects the MB degradation resulting from the photon-induced decomposition effect and can be used to evaluate the photocatalytic activity [4]. This clearly indicates that our Au/TiO_2 nanosols strongly enhance the photocatalytic MB decomposition compared to pure TiO_2.

Single metal oxide semiconductor nanoparticles exhibit in general relatively poor photocatalytic effectiveness. This was attributed to the fact that most photogenerated charge carriers undergo recombination immediately after being generated and are therefore unable to contribute to photocatalysis. Therefore, the Au nanoparticle enhancement of photocatalysis can be explained by assuming that such nanoparticles act as electron traps and promote electron–hole separation [9,24]. The electrons then transfer to adsorbed O_2 acting as electron acceptor to form reactive oxygen radicals finally leading to the MB decomposition.

Effects similar to those for UV radiation were also found for synchrotron X-rays. Fig. 6 shows the visible light spectral changes of MB in de-ionized water in the presence of 0.5 mM of TiO_2 nanosol after different X-ray irradiations. Similar results were obtained when the TiO_2 nanosol was replaced with Au/TiO_2 nanosol (data not shown). The photodegradation ratio C/C_0 (C = remaining methylene blue concentration; C_0 = initial concentration) was derived from the normalized 664 nm peak heights and the results are shown in Fig. 7(a). Compared to the pure TiO_2 nanosol, the Au/TiO_2 nanosol exhibits a slight increase (~5%) of the MB photodegradation in the de-ionized water after X-ray irradiation for 20 s. Similar results are shown in Fig. 7(b) after replacing the de-ionized water with the medium. The Au/TiO_2 nanoparticles in the cell culture medium exhibited a larger enhancement (~11%) compared to de-ionized water after X-ray irradiation. The causes of this difference are still under investigation.

3.3. Colloidal stability analysis and cytotoxicity assay

Good colloidal stability within cellular environments is critical for investigating the interactions between nanoparticles and cells. The evolution of the hydrodynamic size of TiO_2 and Au/TiO_2 nanosols in the RPMI medium or de-ionized water was monitored during up to 4 h by dynamic light scattering and the results are summarized in Table 1. For suspensions in distilled water, the initial average hydrodynamic size of the Au/TiO_2 nanosol was 225.3 nm, which is almost the same as that of the TiO_2 nanosol (239.1 nm). The average hydrodynamic size of TiO_2 nanoparticles increased to ~ 342.5 nm after 4 h of incubation; on the contrary, no such

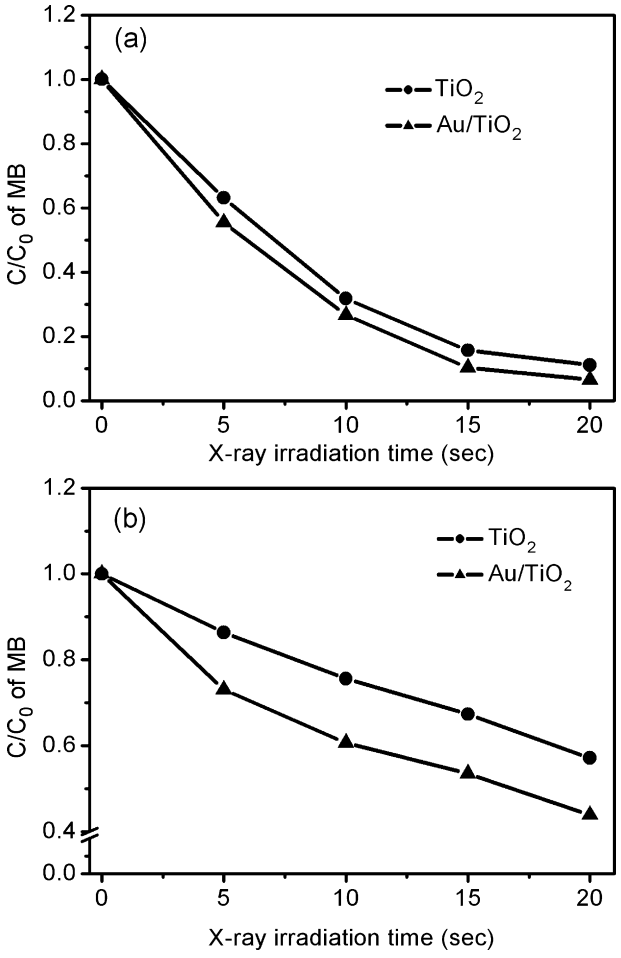

Fig. 7. Photocatalytic MB degradation for TiO_2 and Au/TiO_2 (Au/Ti = 0.050) nanoparticles in (a) de-ionized water and (b) cell culture medium, as a function of the X-ray irradiation time. The initial concentrations were: MB = 0.25 mM; TiO_2 = 0.5 mM; Au/TiO_2 = 0.028 mM/0.5 mM.

increase was observed for Au/TiO_2 nanoparticles whose average size remained almost unchanged (246.2 nm).

For suspensions in cell culture medium, the initial average hydrodynamic size of TiO_2 and Au/TiO_2 nanoparticles (487.2 and 318.7 nm) was large compared to distilled water. The TiO_2 nanoparticle size increased significantly to 635.1 nm after 4 h of incubation, whereas the growth was more limited for Au/TiO_2 nanoparticles (341 nm). All these results indicate that the colloidal stability of Au/TiO_2 nanosol is much better than pure TiO_2 nanosol both in distilled water and in the cell culture medium. The size increase of nanoparticles in the cell culture medium can be explained by protein absorption [25].

Table 1
Hydrodynamic particle mean size for TiO_2 and Au/TiO_2 (Au/Ti = 0.050) nanosols derived from dynamic light scattering results; condition: MB = 0.25 mM; TiO_2 = 0.5 mM; Au/TiO_2 = 0.028 mM/0.5 mM.

Suspension	Actual mean particle size in suspension (nm) Incubating time	
	0 h	4 h
TiO_2 in DI water	225.3	342.5
TiO_2 in medium	487.2	635.1
Au/TiO_2 in DI water	239.1	246.2
Au/TiO_2 in medium	318.1	341

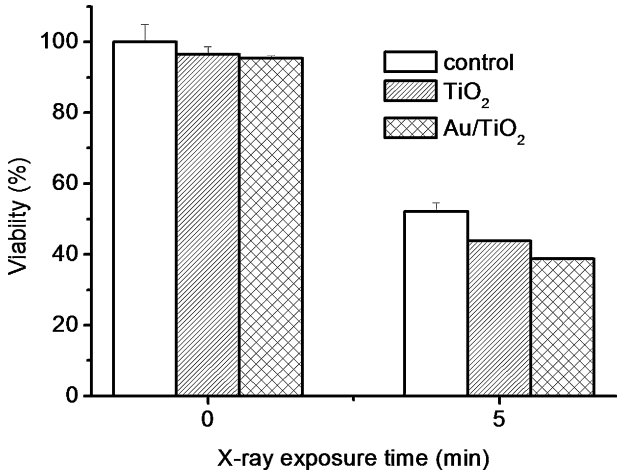

Fig. 8. Cytotoxicity of Au/TiO_2 (Au/Ti = 0.050) nanoparticles for the EMT-6 cell line in the dark and after X-ray irradiation for 5 min.

The cytotoxicity of Au/TiO_2 nanosols for EMT-6 cells was once again assessed by MTT assay. Fig. 8 clearly demonstrates that the introduction of Au/TiO_2 nanoparticles did not affect the mitochondrial function and revealed no cytotoxicity (up to 0.5 mM). In addition, the enhanced cell killing by adding Au nanoparticles to the TiO_2 surface after X-ray exposure could also be observed. For example, after 5 min X-ray exposure, the viability was 43.8 and 38.7% for the cell treated with TiO_2 nanoparticles and Au/TiO_2 nanoparticles.

4. Conclusion

We presented an X-ray radiation synthesis/reduction method that requires no additional reducing agent and no stabilizers to produce well dispersed Au/TiO_2 nanocomposites in aqueous solutions. Gold nanoparticles with controlled size (2–5 nm) were uniformly produced on the surfaces of anatase TiO_2 nanoparticles. The resulting Au/TiO_2 nanoparticles are more effective photocatalysts during X-ray irradiation than unmodified TiO_2 nanoparticles at physiologically relevant concentrations. In addition, the Au/TiO_2 nanosol exhibits sufficient colloidal stability in a cellular environment and is nontoxic with respect to the EMT-6 cell line. Moreover, the enhancement of X-ray irradiation-induced cancer cell-killing effect by Au/TiO_2 nanoparticles is more pronounced to that of bare TiO_2 nanoparticles. These findings could possibly lead to the use of Au/TiO_2 nanoparticles for enhanced radiotherapy.

Acknowledgements

This work was supported by the Biomedical NanoImaging Core Facility, National Science Council (Taiwan), by the Academia Sinica (Taiwan), by Creative Research Initiatives (Functional X-ray Imaging) of MOST/KOSEF, by the Swiss Fonds National de la Recherche Scientifique and by the EPFL.

References

[1] M. Grätzel, J. Photochem. Photobiol. A 164 (2004) 3.
[2] A. Orlov, D.A. Jefferson, N. Macleod, R.M. Lambert, Catal. Lett. 92 (2004) 41.
[3] S. Ivankovic, M. Gotic, M. Jurin, S. Music, J. Sol–Gel Sci. Technol. 27 (2003) 225.
[4] C.Y. Wang, C.Y. Liu, X. Zheng, J. Chen, T. Shen, Colloid. Surf. A 131 (1998) 271.
[5] V. Subramanian, E.E. Wolf, P.V. Kamat, Langmuir 19 (2003) 469.
[6] H.M. Sung-Suh, J.R. Choi, H.J. Hah, S.M. Koo, Y.C. Bae, J. Photochem. Photobiol. A 163 (2004) 37.
[7] A. Sclafani, J.M. Herrmann, J. Photochem. Photobiol. A 113 (1998) 181.
[8] U. Siemon, D. Bhanemann, J.J. Testa, D. Rodrigues, M.I. Litter, N. Bruno, J. Photochem. Photobiol. A 148 (2002) 247.
[9] A. Dawson, P.V. Kamat, J. Phys. Chem. B 105 (2001) 960.
[10] R. Zanella, S. Giorgio, C.R. Henry, C. Louis, J. Phys. Chem. B 106 (2002) 7634.

[11] J.A. Rodriguez, G. Liu, T. Jirsak, J. Hrbek, Z.P. Chang, J. Dvorak, A. Maiti, J. Am. Chem. Soc. 124 (2002) 5242.
[12] J.F. Hainfeld, D.N. Slatkin, H.M. Smilowitz, Phys. Med. Biol. 49 (2004) N309.
[13] D.M. Herold, I.J. Das, C.C. Stobbe, R.V. Iyer, J.D. Chapman, Int. J. Radiat. Biol. 76 (2000) 1357.
[14] Y.C. Yang, C.H. Wang, Y.K. Hwu, J.H. Je, Mater. Chem. Phys. 100 (2006) 72.
[15] C.C. Kim, C.H. Wang, Y.C. Yang, Y.K. Hwu, S.K. Seol, Y.B. Kwon, C.H. Chen, H.W. Liou, H.M. Lin, Mater. Chem. Phys. 100 (2006) 292.
[16] C.H. Wang, C.C. Chien, Y.L. Yu, C.J. Liu, C.F. Lee, C.H. Chen, Y. Hwu, C.S. Yang, J.H. Je, G. Margaritondo, J. Synchrot. Radiat. 14 (2007) 477.
[17] C.H. Wang, T.E. Hua, C.C. Chien, Y.L. Yu, T.Y. Yang, C.J. Liu, W.H. Leng, Y.K. Hwu, Y.C. Yang, C.C. Kim, J.H. Je, C.H. Chen, M.H. Lin, G. Margaritondo, Mater. Chem. Phys. 106 (2007) 323.
[18] R. Cai, Y. Kubota, T. Shuin, H. Sakai, K. Hashimoto, A. Fujishima, Cancer Res. 52 (1992) 2345.
[19] A. Fujishima, N.T. Rao, D.A. Tryk, J. Photochem. Photobiol. C 1 (2000) 1.
[20] C.J. Liu, C.H. Wang, C.L. Wang, Y. Hwu, C.Y. Lin, G. Margaritondo, J. Synchrot. Radiat. 16 (2009) 395.
[21] T.H. Li, H.G. Park, S.H. Choi, Mater. Chem. Phys. 105 (2007) 325.
[22] P.C. Hsu, C.H. Wang, T.Y. Yang, Y.K. Hwu, C.S. Lin, C.H. Chen, L.W. Chang, S.K. Seol, J.H. Je, G. Margaritondo, J. Vac. Sci. Technol. A 25 (2007) 615.
[23] M. Haruta, Catal. Today 36 (1997) 153.
[24] V. Subramanian, E.E. Wolf, P.V. Kamat, J. Am. Chem. Soc. 126 (2004) 4943.
[25] L.K. Limbach, Y. Li, R.N. Grass, T.J. Brunner, M.A. Hintermann, M. Muller, D. Gunther, W. Stark, Environ. Sci. Technol. 39 (2005) 9370.